Xenon Sorption

Deutsche Ausgabe: DOI: 10.1002/ange.201602287
Internationale Ausgabe: DOI: 10.1002/anie.201602287

Hybrid Ultra-Microporous Materials for Selective Xenon Adsorption and Separation

*Mona H. Mohamed[+], Sameh K. Elsaidi[+], Tony Pham, Katherine A. Forrest, Herbert T. Schaef, Adam Hogan, Lukasz Wojtas, Wenqian Xu, Brian Space, Michael J. Zaworotko, and Praveen K. Thallapally**

Abstract: *The demand for Xe/Kr separation continues to grow due to the industrial significance of high-purity Xe gas. Current separation processes rely on energy intensive cryogenic distillation. Therefore, less energy intensive alternatives, such as physisorptive separation, using porous materials, are required. Herein we show that an underexplored class of porous materials called hybrid ultra-microporous materials (HUMs) affords new benchmark selectivity for Xe separation from Xe/Kr mixtures. The isostructural materials, CROFOUR-1-Ni and CROFOUR-2-Ni, are coordination networks that have coordinatively saturated metal centers and two distinct types of micropores, one of which is lined by CrO_4^{2-} (CROFOUR) anions and the other is decorated by the functionalized organic linker. These nets offer unprecedented selectivity towards Xe. Modelling indicates that the selectivity of these nets is tailored by synergy between the pore size and the strong electrostatics afforded by the CrO_4^{2-} anions.*

Xenon (Xe) and Krypton (Kr) separation is of industrial interest because these gases present either commercial value as a commodity or an environmental threat.[1] High-purity Xe gas is valuable because of its applications in imaging, lighting, lasers, and medical science. The existing technology for Xe/Kr separation uses cryogenic distillation, which is energetically demanding and laborious. This was reflected in our recent economic analysis, which suggests that metal–organic framework (MOF) based separation at room temperature could be more cost effective than cryogenic distillation in the context of nuclear reprocessing plants. The radioactive ^{85}Kr and ^{133}Xe can be introduced to the atmosphere during nuclear reprocessing operations, which means that they need to be captured and sequestered safely.[2] Although Xe is generated as fission product, by the time the fuel is reprocessed, all the radioactive isotopes of Xe have decayed to very low concentrations. Radioactive ^{85}Kr has a long half-life ($t_{1/2} = 10.8$ years) and therefore must be captured and removed to prevent its uncontrolled release into the atmosphere. Further presence of any trace amounts of radioactive Kr in Xe rich stream as a byproduct is not suitable for practical use. These factors incentivize the development of an alternative technology for a less energy-intensive, more cost-effective, and safer process to capture Kr and Xe from reprocessing operations. In this regard, Zeolites and activated carbon have been evaluated for Xe/Kr separation at ambient conditions, however their low Xe selectivity and adsorption capacity renders them impractical.[3] Metal–organic materials (MOMs)[4] have also been widely investigated in terms of this gas separation due to their promising features including their inherent structural modularity, extra-large surface area, good thermal stability and recyclability.[5] However, MOMs that rely on unsaturated metal centers have many drawbacks, such as their strong tendency to interact with water and the high energy costs associated with their activation and recyclability. Several theoretical studies suggest that a porous material for Xe adsorption and separations should possess an optimal pore size that is similar to or just above the kinetic diameter of Xe (4.1 Å).[6] A newly designated subclass of MOMs called hybrid ultra-microporous materials (HUMs), which are assembled by saturated metal cites (SMCs), which in turn connected by combinations of organic linkers and inorganic pillars. These HUMs have shown unprecedented performance in the context of CO_2 capture thanks to the combination of optimal pore size and strong electrostatics afforded by the inorganic anions.[7] In essence, HUMs can have the advantages of both zeolites (stability) and MOMs (high modularity, controllable pore size and chemistry). The **mmo** platform is a family of HUMs that is sustained by pillaring square grid sheets ($[M(bpe)_2]^{2+}$; bpe = 1,2-bis(4-pyridyl)ethylene) by angular inorganic pillars, such as CrO_4^{2-}, MoO_4^{2-}, and WO_4^{2-}. These materials are already known to exhibit exceptional properties in terms of CO_2 adsorption and separations.[8] Herein, two microporous **mmo** topology networks, the CROFOUR-1-Ni[8a] prototypal **mmo** network and a new

[*] Dr. M. H. Mohamed,[+] Dr. S. K. Elsaidi,[+] Dr. H. T. Schaef, Dr. P. K. Thallapally
Physical and Computational Science Directorate
Pacific Northwest National Laboratory
Richland, WA 99352 (USA)
E-mail: praveen.thallapally@pnnl.gov
Dr. M. H. Mohamed,[+] Dr. S. K. Elsaidi[+]
Chemistry Department, Faculty of Science, Alexandria University
P.O.Box 426 Ibrahimia, Alexandria 21321 (Egypt)
Dr. T. Pham, K. A. Forrest, A. Hogan, Dr. L. Wojtas, Prof. Dr. B. Space
Department of Chemistry, University of South Florida
4202 East Fowler Ave., CHE205, Tampa, FL 33620 (USA)
Dr. W. Xu
X-ray Science Division, Advanced Photon Source, Argonne National Laboratory
Argonne, IL 60439 (USA)
Prof. Dr. M. J. Zaworotko
Department of Chemical & Environmental Sciences, University of Limerick
Limerick (Republic of Ireland)
[+] These authors contributed equally to this work.

Supporting information for this article can be found under: http://dx.doi.org/10.1002/anie.201602287.

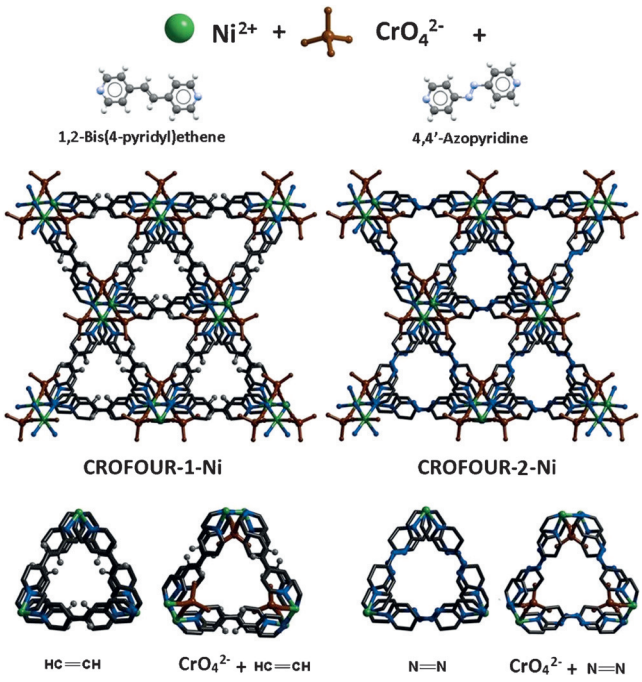

Scheme 1. The formation and structure of **mmo** nets; CROFOUR-1-Ni and CROFOUR-2-Ni, based on the SMCs and CrO_4^{2-} pillars. The bottom row shows the two types of pores in each net: lined by the functionalized organic linker (C=C from bpe or N=N from azp) or the oxygen atoms from the inorganic linkers (two from each CrO_4^{2-}).

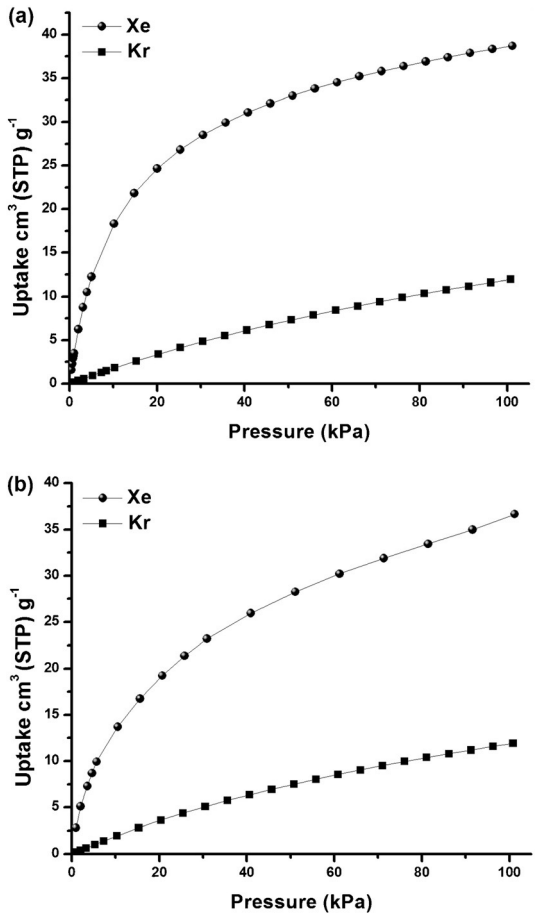

Figure 1. Pure gas adsorption isotherms. a) Single component gas adsorption isotherms for CROFOUR-1-Ni collected at 298 K and b) Single component gas adsorption isotherms for CROFOUR-2-Ni collected at 298 K.

variant, CROFOUR-2-Ni (see Scheme 1), have been investigated for Xe and Kr adsorption and separation by collecting pure gas adsorption isotherms and column breakthrough experiments for various Xe/Kr gas mixtures.

We targeted the **mmo** platform because its hybrid nature enables physicochemical properties that are not readily achieved in existing classes of porous materials and it is modular. Such structures can offer diversity in terms of pore size and chemistry and are amenable to be custom-designed to target a certain function. CROFOUR-2-Ni, $[Ni(azp)_2CrO_4]$ (azp = 4,4′-azopyridine), is a new HUM that is isostructural to the prototypal **mmo** nets CROFOUR-1-Ni, MOFOUR-1-Ni and WOFOUR-1-Ni.[8a,9] CROFOUR-1-Ni and CROFOUR-2-Ni, possess two distinct types of micropores: one is decorated by six oxygen atoms from the inorganic linkers (two from each CrO_4^{2-} moiety); the second is lined by the functionalized organic linker (N=N from azp or C=C from bpe; Scheme 1.

Permanent porosity of CROFOUR-2-Ni was confirmed by CO_2 adsorption measurements collected at 195 K (see Supporting Information) and the Langmuir surface area was found to be 475 $m^2 g^{-1}$. Xe and Kr adsorption isotherms were collected at 298 K, 288 K and 278 K for CROFOUR-1-Ni and CROFOUR-2-Ni. The adsorption isotherms revealed Xe uptakes of 39.6 $cm^3 g^{-1}$ (47.1 $cm^3 cm^{-3}$) and 36 $cm^3 g^{-1}$ (45.7 $cm^3 cm^{-3}$) for CROFOUR-1-Ni and CROFOUR-2-Ni, respectively and Kr uptakes of 11 $cm^3 g^{-1}$ (13.1 $cm^3 cm^{-3}$) and 11.5 $cm^3 g^{-1}$ (14.6 $cm^3 cm^{-3}$) at 298 K and 1 bar, respectively. The total uptake of gases at 1 bar is an important reference point, but it is not necessarily relevant to efficient trace gas separations. Figure 1 reveals the high affinity of Xe over Kr in both materials as exemplified by the steep Xe uptakes at low pressure, that is, conditions that are more pertinent for trace and low-concentration Xe capture and separation.

The isosteric heats of adsorption (Q_{st}) of Xe and Kr gases were calculated by two methods, Clausius–Clapeyron and Langmuir–Freundlich methods, using single adsorption isotherms. To our knowledge, CROFOUR-1-Ni exhibits the highest value for Xe Q_{st} at low loading: 37.4 kJ mol^{-1}. The Q_{st} of Xe in CROFOUR-2-Ni, 30.5 kJ mol^{-1} at low loading (Table 1), which is also higher than most other classes of porous materials including MOMs and activated carbon.

To investigate the practical potential of these materials, column breakthrough experiments were conducted at 298 K for Xe/Kr gas mixtures on CROFOUR-1-Ni and CROFOUR-2-Ni (Figure 2). The separation times between Xe and Kr gases for the 20:80 gas mixture were found to be 39 and 32 min g^{-1} for CROFOUR-1-Ni and CROFOUR-2-Ni, respectively (see Figure 2 and see Supporting Information for 50:50 mixture). These results indicate that these HUMs efficiently adsorb and separate Xe gas with high selectivity.

Ideal adsorbed solution theory (IAST) was used to predict the selectivity of Xe/Kr binary mixtures based on the

Table 1: The adsorption performance parameters of the benchmark porous materials in terms of Xe/Kr separation.

Sorbent	Xe uptake at 1 bar [mmol g^{-1}]	Xe *Qst* [kJ mol^{-1}]	20:80 Xe/Kr Selectivity
Activated Carbon[10]	4.2	6.6	2.9[a]
MOF-74-Ni[10,11]	4.2	22	4[a]
MOF-74-Co[11]	6.1	26.3	10.37[d]/3.91[e]
MOF-74-Mg[11]	5.6	23.5	5.94[d]/3.76[e]
Ag@MOF-74Ni[12]	4.6	NR	11.5[c]
HKUST-1[10,11,13]	3.3	17.5	2.6[a]
$Co_3(HCOO)_6$[12b,14]	2	28	11[c]
SBMOF-2[12b]	2.83	26.4	10[c]
CC3[15]	2.4	31.3	12.5[c]
CROFOUR-1-Ni	1.8	37.4	22[c]/19.8[a]
CROFOUR-2-Ni	1.6	30.5	15.5[c]/14.3[a]

[a] From breakthrough experiment. [b] The ratio of uptakes based on single component isotherms. [c] From IAST calculation. [d] Henry's constant based on single component isotherm. [e] Simulated.

experimental single adsorption isotherms collected at 298 K. Selectivity for a 50:50 Xe/Kr binary gas mixture at 298 K and 1 bar were calculated to be 26 and 16 for CROFOUR-1-Ni and CROFOUR-2-Ni, respectively, 22 and 15.5 for a 20:80 Xe/Kr mixture, respectively and 21.5 and 15 for 10:90 Xe/Kr binary mixture, respectively (see Figure 2 and Supporting Information). These values are superior to existing benchmark porous materials including activated carbon,[10] a porous organic cage CC3,[15] MOF-74-Ni,[10,11] Ag@MOF-74-Ni,[12a] $CO_3(HCOO)_6$,[14] SBMOF-2[12b] and HKUST-1[10,11] (see Table 1). Based on our breakthrough experiments using 400 ppm Xe, 40 ppm Kr balanced with air, CC3 outperforms all materials herein. However, IAST calculations indicate that CRFOUR-1-Ni has higher selectivity. The better performance of CC3 is likely the result of its higher adsorption capacity.

Molecular simulations of Xe and Kr adsorption were performed to elucidate the nature of the binding sites in these materials (see Supporting Information for details). The simulations revealed that the primary adsorption site for Xe in both MOMs is located in the cage that contains three CrO_4^{2-} ions in proximity to each other. Xe atoms interact with six terminal oxygen atoms simultaneously (two each from three different CrO_4^{2-} moieties; Figure 3). In both HUMs, the pore size is slighter larger than the kinetic diameter of Xe and provides a favorable fit for the adsorbed Xe atoms. This could explain why the Q_{st} for Xe is exceptionally high. The primary adsorption site for Kr in both MOMs is the same as that for Xe (see Supporting Information). However, interactions between Kr and the moieties at this site in both materials are weaker, presumably due to the smaller polarizability of Kr.[11] The next favorable adsorption site for Kr in both MOMs is the region between two oxygen atoms from two different CrO_4^{2-} groups, which is located next to the primary binding site (see Supporting Information).[16] Adsorption of Xe at this site in the case of CROFOUR-1-Ni is also possible according to the modeling studies. The simulations also revealed that the Xe and Kr atoms can adsorb within the cage that is adjacent to the cage containing the primary binding site in the [001] direction (see Supporting Information). To further support our molecular simulation data, in situ powder XRD measurements were performed on Xe/Kr-adsorbed CROFOUR-1-Ni to locate the gas molecule sites

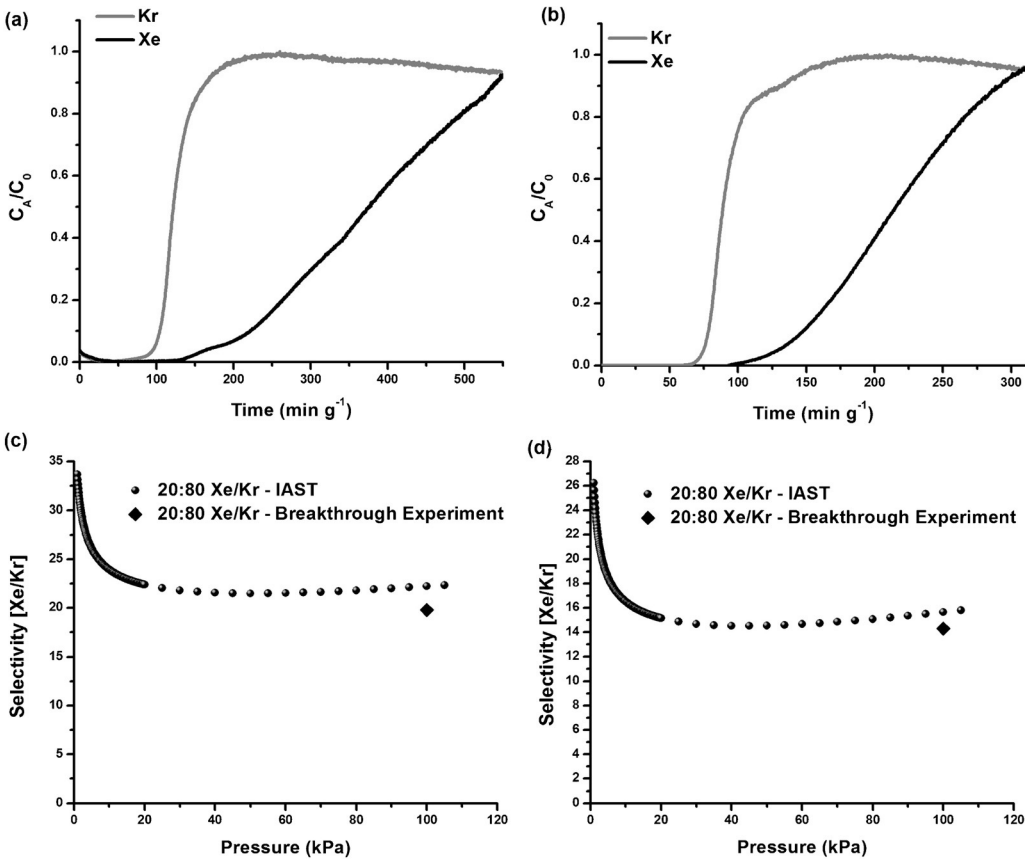

Figure 2. Gas mixture breakthrough experiments and calculated selectivity. a) Column breakthrough experiment for 20:80 Xe/Kr gas mixture at 298 K and 1 bar for CROFOUR-1-Ni, b) same for CROFOUR-2-Ni, c) IAST calculated selectivity for 20:80 Xe/Kr gas mixture compared to the experimental value from the breakthrough experiment at 1 bar for CROFOUR-1-Ni and d) same for CROFOUR-2-Ni.

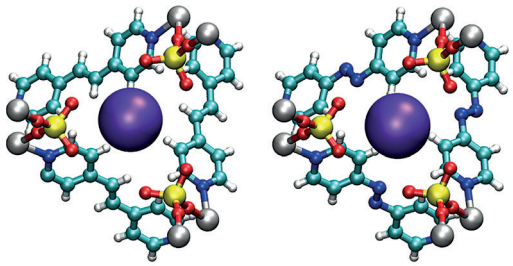

CROFOUR-1-Ni CROFOUR-2-Ni

Figure 3. Illustration of the adsorbed Xe atom (violet) at the primary binding site in CROFOUR-1-Ni (left) and CROFOUR-2-Ni (right) as determined from simulation. The primary binding site is located within the cage that is enclosed by three CrO_4^{2-} ions, where the adsorbate interacts with six terminal oxygen atoms (two from three different CrO_4^{2-} moieties) simultaneously. Atom colors: C cyan, H white, N blue, O red, Cr yellow, Ni silver.

experimentally. The results are in good agreement with the molecular simulations (see Supporting Information for details).[12b] Molecular modelling experiments using Vienna ab initio Simulation Package (VASP) were undertaken to address the co-adsorption of Xe and Kr (Supporting Information for details). The calculated energies of the optimized adsorbate positions revealed a deeper energy basin for the adsorbed Xe, with a difference in energy of approximately 12 kJ mol^{-1} between Xe and Kr for both CROFOUR-1-Ni and CROFOUR-2-Ni. This is consistent with adsorbate selection based on energetic favorability, with the Xe atoms, which out-competes Kr atoms for the binding sites in these HUMs.

In conclusion, two hybrid ultra-microporous materials, CROFOUR-1-Ni and CROFOUR-2-Ni, which are based upon SMCs and CrO_4^{2-} inorganic anions, exhibit adsorption and separation performance towards Xe that surpass benchmark porous materials in this context. These results were supported by column breakthrough experiments for Xe/Kr gas mixtures and validated by molecular simulations. Further work will focus on systematic evaluation of the effect of pore size and functionality on the Xe/Kr adsorption performance of other **mmo** nets.

Acknowledgements

B.S. acknowledges the National Science Foundation (Award No. CHE-1152362), including support from the Major Research Instrumentation Program (Award No CHE-1531590), the computational resources that were made available by a XSEDE Grant (No. TG-DMR090028), and the use of the services provided by Research Computing at the University of South Florida. We (P.K.T) thank the US Department of Energy (DOE), Office of Nuclear Energy for adsorption and breakthrough measurements. We (P.K.T) particularly thank J. Bresee, K. Gray, T. Todd (Idaho National Laboratory), John Vienna (PNNL), B. Jubin (Oak Ridge National Laboratory), and D. M. Strachan (Strachan LLC) for providing programmatic support and guidance. Pacific Northwest National Laboratory is a multi-program national laboratory operated for the US Department of Energy by Battelle Memorial Institute under Contract DE-AC05-76RL01830. M.J.Z. gratefully acknowledges Science Foundation Ireland (Award 13/RP/B2549) for support. This research used Beamline 17-BM of the Advanced Photon Source, a U.S. Department of Energy (DOE) Office of Science User Facility operated for the DOE Office of Science by Argonne National Laboratory under Contract No. DE-AC02-06CH11357.

Keywords: chromium · hybrid ultra-microporous materials · metal–organic frameworks · separations · xenon

How to cite: *Angew. Chem. Int. Ed.* **2016**, *55*, 8285–8289
Angew. Chem. **2016**, *128*, 8425–8429

[1] D. Banerjee, A. J. Cairns, J. Liu, R. K. Motkuri, S. K. Nune, C. A. Fernandez, R. Krishna, D. M. Strachan, P. K. Thallapally, *Acc. Chem. Res.* **2015**, *48*, 211–219.
[2] J. P. Fontaine, F. Pointurier, X. Blanchard, T. Taffary, *J. Environ. Radioact.* **2004**, *72*, 129–135.
[3] a) C. J. Jameson, A. K. Jameson, L. Hyung-Mi, *J. Chem. Phys.* **1997**, *107*, 4364; b) K. F. Chackett, D. G. Tuck, *Trans. Faraday Soc.* **1957**, *53*, 1652–1658.
[4] a) S. Kitagawa, R. Kitaura, S.-i. Noro, *Angew. Chem. Int. Ed.* **2004**, *43*, 2334–2375; *Angew. Chem.* **2004**, *116*, 2388–2430; b) H. Furukawa, K. E. Cordova, M. O'Keeffe, O. M. Yaghi, *Science* **2013**, *341*, 1230444–1230444; c) H.-C. Zhou, J. R. Long, O. M. Yaghi, *Chem. Rev.* **2012**, *112*, 673–674; d) G. Férey, *Chem. Soc. Rev.* **2008**, *37*, 191–214.
[5] a) O. K. Farha, I. Eryazici, N. C. Jeong, B. G. Hauser, C. E. Wilmer, A. A. Sarjeant, R. Q. Snurr, S. T. Nguyen, A. O. Yazaydin, J. T. Hupp, *J. Am. Chem. Soc.* **2012**, *134*, 15016–15021; b) V. Guillerm, F. Ragon, M. Dan-Hardi, T. Devic, M. Vishnuvarthan, B. Campo, A. Vimont, G. Clet, Q. Yang, G. Maurin, G. Férey, A. Vittadini, S. Gross, C. Serre, *Angew. Chem. Int. Ed.* **2012**, *51*, 9267–9271; *Angew. Chem.* **2012**, *124*, 9401–9405; c) M. Eddaoudi, J. Kim, N. Rosi, D. Vodak, J. Wachter, M. O'Keeffe, O. M. Yaghi, *Science* **2002**, *295*, 469–472.
[6] a) C. M. Simon, R. Mercado, S. K. Schnell, B. Smit, M. Haranczyk, *Chem. Mater.* **2015**, *27*, 4459–4475; b) B. J. Sikora, C. E. Wilmer, M. L. Greenfield, R. Q. Snurr, *Chem. Sci.* **2012**, *3*, 2217.
[7] a) P. Nugent, Y. Belmabkhout, S. D. Burd, A. J. Cairns, R. Luebke, K. Forrest, T. Pham, S. Ma, B. Space, L. Wojtas, M. Eddaoudi, M. J. Zaworotko, *Nature* **2013**, *495*, 80–84; b) S. K. Elsaidi, M. H. Mohamed, H. T. Schaef, A. Kumar, M. Lusi, T. Pham, K. A. Forrest, B. Space, W. Xu, G. J. Halder, J. Liu, M. J. Zaworotko, P. K. Thallapally, *Chem. Commun.* **2015**, *51*, 15530–15533.
[8] a) M. H. Mohamed, S. K. Elsaidi, L. Wojtas, T. Pham, K. A. Forrest, B. Tudor, B. Space, M. J. Zaworotko, *J. Am. Chem. Soc.* **2012**, *134*, 19556–19559; b) S. D. Burd, P. S. Nugent, M. H. Mohamed, S. K. Elsaidi, M. J. Zaworotko, *Chimia* **2013**, *67*, 372–378.
[9] M. H. Mohamed, S. K. Elsaidi, T. Pham, K. A. Forrest, B. Tudor, L. Wojtas, B. Space, M. J. Zaworotko, *Chem. Commun.* **2013**, *49*, 9809–9811.
[10] J. Liu, P. K. Thallapally, D. Strachan, *Langmuir* **2012**, *28*, 11584–11589.
[11] J. J. Perry, S. L. Teich-McGoldrick, S. T. Meek, J. A. Greathouse, M. Haranczyk, M. D. Allendorf, *J. Phys. Chem. C* **2014**, *118*, 11685–11698.
[12] a) J. Liu, D. M. Strachan, P. K. Thallapally, *Chem. Commun.* **2014**, *50*, 466–468; b) X. Chen, A. M. Plonka, D. Banerjee, R.

Krishna, H. T. Schaef, S. Ghose, P. K. Thallapally, J. B. Parise, *J. Am. Chem. Soc.* **2015**, *137*, 7007 – 7010.
[13] A. Soleimani Dorcheh, D. Denysenko, D. Volkmer, W. Donner, M. Hirscher, *Microporous Mesoporous Mater.* **2012**, *162*, 64 – 68.
[14] H. Wang, K. Yao, Z. Zhang, J. Jagiello, Q. Gong, Y. Han, J. Li, *Chem. Sci.* **2014**, *5*, 620.
[15] L. Chen, P. S. Reiss, S. Y. Chong, D. Holden, K. E. Jelfs, T. Hasell, M. A. Little, A. Kewley, M. E. Briggs, A. Stephenson, K. M. Thomas, J. A. Armstrong, J. Bell, J. Busto, R. Noel, J. Liu, D. M. Strachan, P. K. Thallapally, A. I. Cooper, *Nat. Mater.* **2014**, *13*, 954 – 960.
[16] S. K. Ghose, Y. Li, A. Yakovenko, E. Dooryhee, L. Ehm, L. E. Ecker, A. C. Dippel, G. J. Halder, D. M. Strachan, P. K. Thallapally, *J. Phys. Chem. Lett.* **2015**, *6*, 1790 – 1794.

Received: March 5, 2016
Revised: April 26, 2016
Published online: May 30, 2016

